TISSUE ENGINEERING: Part C
Volume 20, Number 10, 2014

DOI: 10.1089/ten.tec.2013.0518

Patterning Expression of Regenerative Growth Factors Using High Intensity Focused Ultrasound

Christopher G. Wilson, PhD,[1] Francisco M. Martín-Saavedra, PhD,[1–3] Frédéric Padilla, PhD,[4,5] Mario L. Fabiilli, PhD,[4] Man Zhang, PhD,[4] Alexander M. Baez, BS,[4] Christopher J. Bonkowski,[1] Oliver D. Kripfgans, PhD,[4] Richard Voellmy, PhD,[6,7] Nuria Vilaboa, PhD,[2,3] J. Brian Fowlkes, PhD,[4,8] and Renny T. Franceschi, PhD[1,8,9]

Temporal and spatial control of growth factor gradients is critical for tissue patterning and differentiation. Reinitiation of this developmental program is also required for regeneration of tissues during wound healing and tissue regeneration. Devising methods for reconstituting growth factor gradients remains a central challenge in regenerative medicine. In the current study we develop a novel gene therapy approach for temporal and spatial control of two important growth factors in bone regeneration, vascular endothelial growth factor, and bone morphogenetic protein 2, which involves application of high intensity focused ultrasound to cells engineered with a heat-activated- and ligand-inducible gene switch. Induction of transgene expression was tightly localized within cell-scaffold constructs to subvolumes of $\sim 30\,mm^3$, and the amplitude and projected area of transgene expression was tuned by the intensity and duration of ultrasound exposure. Conditions for ultrasound-activated transgene expression resulted in minimal cytotoxicity and scaffold damage. Localized regions of growth factor expression also established gradients in signaling activity, suggesting that patterns of growth factor expression generated by this method will have utility in basic and applied studies on tissue development and regeneration.

Introduction

Temporally- and spatially restricted patterns of growth factor distribution are critical for the development of all tissues. For example, in long bone formation vascular endothelial growth factor (VEGF) is initially concentrated at the margins of the limb anlagen, shifts to the diaphysis during elongation of the presumptive bone, and at later times is associated with the hypertrophic zone of epiphyseal chondrocytes.[1] Concentration gradients of bone morphogenetic proteins (BMPs), including BMPs 2, 4, and 7, also provide essential patterning signals in the developing limb.[2,3] Similar programs of growth factor expression are also re-initiated during normal fracture healing.[4–6] A major challenge for regenerative medicine is to reconstitute these developmental patterns of growth factor distribution to stimulate new tissue formation.

In the area of musculoskeletal tissue regeneration, gene therapies using BMP-encoding vectors (e.g., plasmids or viruses) or cells engineered to express BMPs demonstrated robust healing capacity in animal models of critical-sized bone defects.[7–9] Implantation of cells engineered with ligand-regulated BMP expression systems also exhibited osteogenic activity *in vivo* and additionally afforded tight temporal control over transgene expression.[10,11] However, methods for achieving combined spatial and temporal control over the expression of regenerative transgenes have not been reported, yet may be crucial for localizing the osteogenic response and reducing heterotopic ossification and other systemic toxicities that can arise from uncontrolled BMP release.[12–14]

We recently reported on the construction and operation of a novel synthetic gene switch activated by thermal stress and dependent on a small molecule ligand (rapamycin, or related

[1]Department of Periodontics and Oral Medicine, Center for Craniofacial Regeneration, University of Michigan School of Dentistry, Ann Arbor, Michigan.
[2]Hospital Universitario La Paz-IdiPAZ, Madrid, Spain.
[3]CIBER de Bioingenieria, Biomateriales y Nanomedicina, CIBER-BBN, Spain.
[4]Department of Radiology, University of Michigan Medical School, Ann Arbor, Michigan.
[5]Claude Bernard Lyon 1 University and INSERM Unit 1032, Lyson Cedex, France.
[6]Department of Physiological Sciences, University of Florida, Gainesville, Florida.
[7]HSF Pharmaceuticals S.A., La Tour-de-Peilz, Switzerland.
[8]Department of Biomedical Engineering, University of Michigan College of Engineering, Ann Arbor, Michigan.
[9]Department of Biological Chemistry, University of Michigan Medical School, Ann Arbor, Michigan.

analogs) to induce transgene expression.[15] By using this gene switch, it was possible to control both the timing and spatial distribution of VEGF. Exposure to a thermal stress delivered by a hyperthermic water bath in the presence of ligand was sufficient to trigger VEGF production for 5–8 days. Further, cells harboring the gene switch were readily reactivated *in vivo* up to a month following implantation indicating tight and reproducible temporal control over transgene expression in the targeted anatomical region. Clinical translation of the aforementioned approach, however, is currently limited in terms of achieving tight spatial and temporal control of gene activation because of an inability to localize the thermal stimulus.

Focused ultrasound is an emerging clinical technology primarily used for the thermal and/or mechanical ablation of cancerous or precancerous tissues deep within the body (e.g., uterine fibroids and prostate cancer). Using this approach, ultrasound energy can be focused to small volumes and generate spatially-restricted regions of hyperthermia. In current clinical applications, image-guided hyperthermia is achieved by coupling a magnetic resonance imaging (MRI) instrument to an integrated high intensity focused ultrasound (HIFU) transducer.[16,17]

Here, we combine the ability of HIFU to spatially control a thermal stimulus with the heat and ligand-dependent gene expression system described above to achieve spatial and temporal control over the production of two important factors involved in bone development and regeneration, VEGF and BMP2. It is envisioned that this novel application of focused ultrasound will provide the spatial and temporal control over transgene expression necessary to reconstitute morphogenic signals capable of guiding the regeneration of bone and other tissues.

Materials and Methods

Gene switch plasmid construction and development of stable cell lines

Construction and evaluation of heat-activated and rapamycin-dependent gene switches (Fig. 1A) for regulating firefly luciferase (*fLuc*) or human VEGF 165 ($hVEGF_{165}$) were reported elsewhere.[15] C3H10T½-TA clone, stably expressing the transactivator component of the heat-activated rapamycin-dependent gene switch was derived from the multipotent murine progenitor cell line C3H10T½ (ATCC). The pLH-Z12l-PL-BMP2 vector[11] containing the entire coding sequence of rat *BMP2* cDNA was transfected into C3H10T½-TA cells using Lipofectamine 2000 (Invitrogen) according to the manufacturer's instructions. Clones were selected using hygromycin B (600 μg/mL) and screened for BMP2 secretion 24 h after treatment with 10 nM rapamycin (LC Laboratories) and subsequent submersion in a 45°C water bath for 30 min. BMP2 secretion was assayed in cell culture supernatants using a specific ELISA kit (R&D Systems). A highly inducible clone that exhibited negligible levels of BMP2 secretion after heat treatment or rapamycin alone was isolated and termed C3H10T½-BMP2. For propagation and selection, cells were cultured in a basal medium composed of high glucose Dulbecco's modified Eagle's medium (DMEM; Invitrogen) with 10% (v/v) fetal bovine serum (FBS; Hyclone), 10 mM HEPES buffer, 100 U/mL penicillin, 100 μg/mL streptomycin, and 50 μg/mL gentamicin.

Evaluation of heat shock- and ligand-inducible BMP2 expression in cell-fibrin constructs

C3H10T½-BMP2 cells were evaluated for heat shock- and ligand-inducible expression of BMP2 using three-

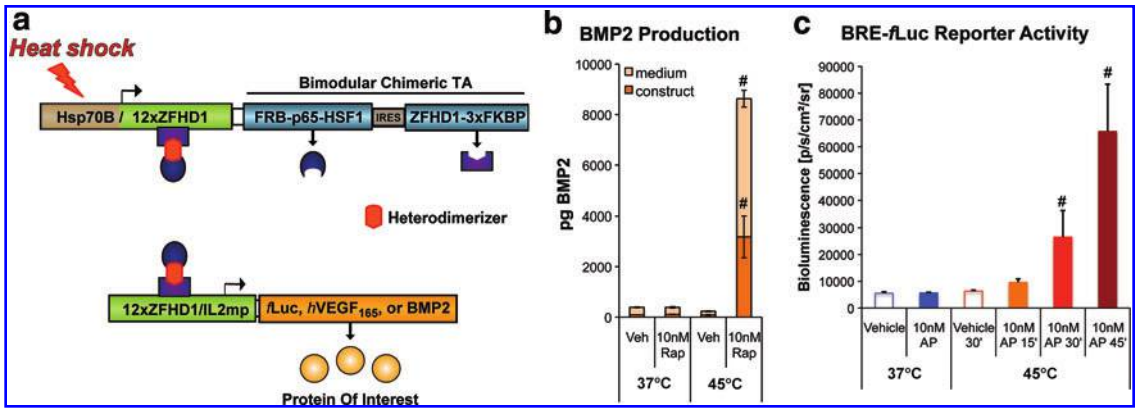

FIG. 1. Development of a heat shock protein (HSP)-based and rapamycin-dependent gene switch for control of BMP2 expression. **(a)** Gene switch design. The first component of the gene switch comprises a human HSP70B promoter that drives expression of a bimodular synthetic transactivator (TA). One module contains the FRB rapamycin-binding domain (derived from human FRAP) and transcriptional activation domains from the p65 subunit of NF-κB and heat shock factor 1 (HSF1). The second module contains FKBP rapamycin-binding domains and zinc finger homeodomain 1 (ZFHD1) DNA-binding domains. In the presence of a dimerizer, the TA autoactivates its own expression through ZFHD1 elements and also drives expression of a transgene of interest [firefly luciferase (*f*Luc), human $VEGF_{165}$, BMP2] *via* the second component of the gene switch. **(b)** BMP2 induction requires heat shock and rapamycin/rapalog treatment. C3H10T½-BMP2 cells were suspended in a fibrin scaffold and exposed to vehicle, 10 nM rapamycin (Rap), and/or a 30 min 45°C hyperthermic stimulus as indicated. BMP2 was measured in the conditioned medium ("medium") and lysates ("construct") of the cell-scaffold constructs. $^{\#}p < 0.05$ versus vehicle and 37°C controls. Data are mean ± standard deviation with $n = 4$. **(c)** BMP Responsive Element (BRE) *f*Luc reporter cell assay. Cells were activated as in **b** except that the rapalog, AP21967 (AP), was used in place of Rap. Conditioned media were obtained from each condition and added to the BRE luciferase BMP reporter cell line. $^{\#}p < 0.05$ versus vehicle and 37°C controls. Data are mean ± standard deviation with $n = 4$. Color images available online at www.liebertpub.com/tec

dimensional (3D) culture assays. A fibrin scaffold was chosen for these studies because it is approved for clinical use in the United States by the Food and Drug Administration (FDA), cells can be uniformly distributed throughout the scaffold, and the mechanical and acoustic properties of the scaffold can be easily tuned by altering the concentration of fibrin precursors. To prepare the cell-fibrin constructs, an appropriate number of cells was first suspended in one volume of ice-cold 20 U/mL bovine thrombin (Sigma-Aldrich) dissolved in DMEM. Next, four volumes of ice-cold DMEM were added to the cell suspension, and finally five volumes of ice-cold bovine fibrinogen dissolved in DMEM (20 mg clottable protein/mL; Sigma-Aldrich) were added to the cell suspension. The fibrinogen solution also contained 0.1 U/mL bovine lung aprotinin (Sigma-Aldrich) to limit degradation of the scaffold. After briefly pipetting to ensure uniform dispersion of the cells, the suspension was distributed among the wells of 16-well chamber slides (Thermo Scientific Nunc) at 200 μL per well and then warmed to 37°C in a tissue culture incubator for 30 min. The final composition of the cell-fibrin constructs was 10^6 cells/mL, 2 U/mL thrombin, 10 mg clottable protein/mL, and 0.05 U/mL aprotinin. Once polymerized, the constructs were removed from the wells of chamber slides and placed in non tissue culture-treated 48-well culture dishes (Thermo Scientific Nunc) with 1 mL of basal medium per construct. For reporter assays (see section, ''Quantification of transgene expression in cell fibrin constructs''), the constructs were cultured in a low-serum (0.1% FBS) variant of the basal medium. Subsets of constructs were incubated with basal medium containing 10 nM rapamycin or 10 nM AP21967, a nonimmunosuppressive rapamycin analog (''rapalog'') kindly provided by ARIAD Pharmaceuticals. Vehicle controls were incubated with medium containing equivalent quantities of carrier solvent ($3–12\times10^{-4}$% v/v dimethylacetamide). After incubation with vehicle or dimerizer for 4 h, the constructs were subjected to a normothermic or a hyperthermic stimulus by floating the culture plates containing the constructs on a 37°C or 45°C water bath, respectively, for 15–45 min. Following thermal activation, culture plates were returned to a standard tissue culture incubator. After 48 h, conditioned media were collected and constructs were minced in five volumes of RIPA buffer. Construct lysates were centrifuged at 15,000 *g* for 15 min and the supernatants and conditioned media were assayed for BMP2 uisng a specific ELISA kit (R&D Systems).

The bioactivity of secreted BMP2 was assessed using a BMP responsive element (BRE) reporter cell line (C3H-B12 cells) kindly provided by Dr D. Logeart-Avramoglou (Paris, CNRS, France). These cells selectively express *fLuc* in response to ng/mL concentrations of BMPs and exhibit low background levels of *fLuc* activity when cultured in low serum-containing media.[18] Cells were plated in 24-well culture dishes at 1.25×10^4 cells/cm^2 in basal medium containing 10% FBS. The following day, cells were rinsed with serum-free DMEM and incubated with undiluted conditioned media collected from induced and noninduced cell-fibrin constructs. After 1 day of incubation with conditioned media, *fLuc* expression was measured by bioluminescence imaging (BLI): cell membrane-permeable D-luciferin substrate (Promega) was added to the media at a final concentration of 80 μg/mL and 30 min later the luminescence signal was captured on an IVIS Spectrum instrument (Perkin-Elmer) in the University of Michigan Small Animal Imaging Core. Quantitative image analysis was performed using the proprietary Living Image software version 4.0 (Perkin-Elmer).

Focused ultrasound-induced hyperthermia

A custom benchtop apparatus was used to deliver focused ultrasound energy to fibrin scaffolds and cell-fibrin constructs (Fig. 2A). The fibrin scaffolds were cast in a six-well culture dish (Bioflex, Flexcell International) modified to have acoustically transparent tops and bottoms. The silastic membrane on the bottom of each well was removed under aseptic conditions and replaced with a sterile Tegaderm membrane (3M). Once the scaffolds or constructs were polymerized within the wells, an autoclaved acrylic annular platen (Flexcell International) was fit into the top of each well. The wells were then filled with basal medium with 10 nM rapamycin and sealed with a second Tegaderm

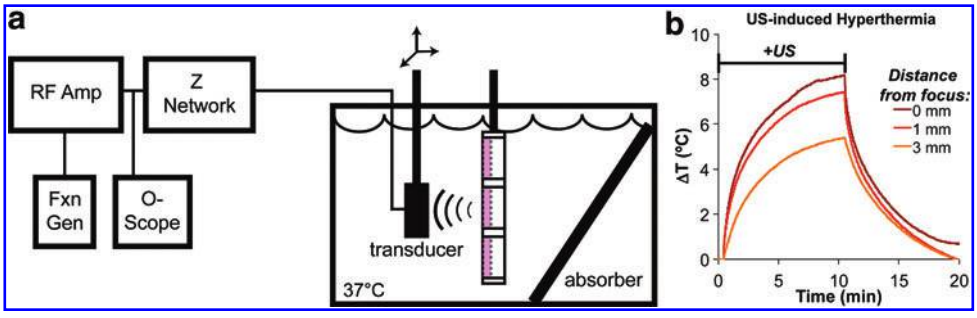

FIG. 2. Application of focused ultrasound to cell-fibrin constructs and induction of localized, mild hyperthermia. **(a)** Apparatus for delivering focused ultrasound to cell-fibrin constructs. Circuitry for driving the ultrasound transducer is shown on the left, including a function generator (Fxn Gen), an RF amplifier (RF Amp), and an impedance matching network (Z Network). A digital oscilloscope (O-scope) was used to monitor the quality of the driving signal. On the right is the tank filled with degassed 37°C water and a six-well Bioflex dish with fibrin scaffolds or cell-fibrin constructs positioned near the focus of the transducer. An absorber limits reflection of ultrasound energy into the samples. **(b)** Time course of temperature rises within a fibrin scaffold upon exposure to continuous wave ultrasound of $I_{SPTA} = 658$ W/cm^2. Temperature measurements were made once per second at the indicated distances from the ultrasound focus using a thermocouple. Color images available online at www.liebertpub.com/tec

membrane to allow for immersion of the dish in the water tank. In all cases, the scaffold precursor solutions and culture media were degassed by vacuum filtration or incubation under house vacuum immediately prior to placement in the culture dish.

The Bioflex dish was fixtured perpendicular to the longitudinal axis of a focused ultrasound transducer in a tank filled with degassed 37°C water. A 2.5 MHz single-element transducer (H-108; SonicConcepts) with a nominal focal width of 0.8 mm and axial focal length of 4 mm (both dimensions, full width at half maximum) was used for these studies. The continuous wave driving signal was generated by an HP3314A function generator (Agilent Technologies) and amplified by a 55 dB radiofrequency (RF) amplifier (A-300; ENI). An impedance matching network (SonicConcepts) was used to improve the efficiency of power delivery to the transducer, and input waveforms were monitored with an oscilloscope (LeCroy). The focus of the ultrasound beam was manually localized within the fibrin scaffold by detecting abrupt increases in temperature using an implanted thermocouple. To accomplish this, a 25G needle (Becton Dickinson) was fixtured through a sidewall of a well in the culture dish. A needle-type thermocouple (Hypo-1; Omega Engineering) was then inserted through the 25G needle and thereby embedded in the scaffold. Temperatures were recorded using a thermocouple data logger (TC-08; Pico Technology) and a laptop computer running PicoLog data acquisition software (Pico Technology).

For activation of cells by focused ultrasound, C3H10T½-*f*Luc that stably harbors an *fLuc* reporter gene under control of the gene switch,[15] or C3H10T½-BMP2 cells were suspended in a fibrin scaffold at 10^6 cells/mL as described above. In some experiments, C3H10T½-TA cells were transiently co-transfected with plasmid pLHZ12-*h*VEGF$_{165}$ and pZ12-*f*Luc[15] at a 1:1 molar ratio using Lipofectamine 2000. Cell-fibrin constructs prepared for confocal microscopy were doped with 75 μg/mL AlexFluor647-fibrinogen (Invitrogen). Constructs of 5 mL volume were cast in the wells of a modified Bioflex dish, allowed to polymerize, and incubated overnight in basal medium containing 10 nM rapamycin. The Bioflex plate containing the cell-fibrin constructs was then immersed in the acoustic exposure tank and allowed to equilibrate to 37°C for ≥30 min. The transducer was positioned to locate the acoustic focus halfway through the thickness of the cell-fibrin construct. Up to nine ultrasound exposures of 5–20 min in duration were performed on each construct, with each exposure spaced laterally 3–4 mm apart. The applied acoustic field at the focus for each exposure ranged from a spatial peak time average intensity (I_{SPTA}) of 658–850 W/cm^2. The corresponding peak compressional and peak rarefactional pressures (P_C/P_R) for these intensities were 5.2/-4.2–6.1/-4.7 MPa as measured with a membrane hydrophone (Reference Shock Wave, Unisyn Medical Technologies) during preliminary calibration experiments. All exposures were performed at the transducer's fundamental frequency of 2.5 MHz, and the resulting pressure waveforms exhibited <2% total harmonic distortion over the range of driving voltages used in these studies. After applying ultrasound, the constructs were aseptically transferred to 60 mm culture dishes with 15 mL basal medium containing 10 nM rapamycin and incubated overnight.

Quantification of transgene expression in cell-fibrin constructs

The expression of *f*Luc in C3H10T½ -*f*Luc-populated constructs was measured by BLI 24 h following exposure to focused ultrasound essentially as described above. For evaluation of BMP2 or *h*VEGF expression in cell-fibrin constructs, ultrasound-exposed portions of the constructs were extracted using a 6 mm diameter punch. The extracted plugs were moved to the wells of a 48-well culture dish with basal medium containing 10 nM rapamycin and incubated for 48 h. The quantity of growth factor in conditioned medium and construct lysates was measured by commercially available ELISAs for BMP2 or *h*VEGF (R&D Systems). The bioactivity of BMP2 in ultrasound-exposed C3H10T½-BMP2-populated constructs was assessed by plating BRE reporter cells on top of the constructs at 2.5×10^4 cells/cm^2 24 h after ultrasound exposure. Co-cultures were then incubated for 48 h in low-serum (0.1% FBS) medium with 10 nM rapamycin and *f*Luc activity was measured by BLI following the procedure described above. BRE reporter activity (as indicated by bioluminescent signal) was calibrated against treatment with known concentrations of *rh*BMP2 (R&D Systems) in cell monolayers cultured at similar cell densities and for equivalent durations in 24-well culture dishes.

Assessment of cell viability and scaffold morphology

The viability of cells encapsulated in fibrin scaffolds exposed to focused ultrasound was evaluated using the alamarBlue assay (Invitrogen), which measures cellular reducing activity. Activated regions of C3H10T½-*f*Luc-populated constructs were identified by BLI and extracted using a 6 mm biopsy punch (Miltex). The extracted plugs were moved to the wells of a 48-well culture dish with 500 μL basal medium containing 10% (v/v) alamarBlue reagent. Following incubation for 2 h, the conditioned media were collected and alamarBlue dye reduction was assayed by measuring fluorescence at $\lambda_{ex} = 550$ nm and $\lambda_{em} = 590$ nm on a Gemini Spectramax fluorescence plate reader (Molecular Devices). A subset of extracted plugs from AlexaFluor647-fibrinogen-doped constructs were incubated with 10 μM CellTracker Green (5-chloromethylfluorescein diacetate, CMFDA; Invitrogen) for 1 h in basal medium, rinsed twice with phosphate buffered saline, and fixed in 4% paraformaldehyde for 12 h at 4°C. After fixation the stained plugs were mounted in coverwell imaging chambers (Electron Microscopy Sciences) with PBS and imaged on a Nikon A1 confocal microscope (Nikon Instruments) with a 10× objective and 488 and 640 nm diode lasers.

In vivo *activation of a heat shock- and ligand-inducible gene switch with focused ultrasound*

All procedures were approved by the University Committee on the Use and Care of Animals and were in compliance with state and federal laws. In preparation for implantation of cell-fibrin constructs and subsequent ultrasound exposures, the backs of male C3H mice were shaved and treated with a depilatory cream. C3H10T½-*f*Luc cells were suspended in a fibrinogen/DMEM solution and kept on ice. Immediately prior to injection, the cell suspension was

mixed with an ice-cold solution of thrombin, rapamycin, and DMEM. Injections of 500 μL/implant were placed lateral to the spine (one on each side) through a 20G needle (Becton Dickinson) and allowed to polymerize for 3 h. The final concentrations of cells, fibrinogen, thrombin, and rapamycin in each implant were 10^6/mL, 10 mg/mL, 2 U/mL, and 50 nM, respectively. To apply focused ultrasound to the implants, mice were anesthesized with isofluorane and immobilized in a 37°C water bath such that the lower back of each animal was submerged. A single element focused ultrasound transducer (Sonic Concepts) fit with a water coupling cone was manually aimed at some implants with the focus positioned within the implant and the longitudinal axis of the focal volume approximately orthogonal to the skin. A continuous 2.5 MHz driving signal for the transducer was generated by an HP3314A function generator and amplified by a 50 dB RF amplifier (240 L, ENI). Implants were treated with $I_{SATA} = 0$ or 658 W/cm^2 ultrasound for 10 min. Following application of the ultrasound, mice were returned to their cages and imaged for bioluminescence the following day. Briefly, 50 μL of 40 mg/mL D-luciferin substrate in sterile PBS was injected into each implant and the mice were immediately placed in the BLI instrument for imaging. The mice were then returned to their cages and sacrificed the following day. The implants and overlying skin were resected, fixed in 10% neutral buffered formalin, embedded in paraffin, sectioned to 5 μm, deparaffinized, and stained with hematoxylin and eosin. Sections of implants from control and irradiated regions were then imaged on an Eclipse Ti microscope (Nikon Instruments) with a 4× objective.

Statistics

Data were analyzed by the general linear model and Tukey's *post-hoc* tests for multiple comparisons using SPSS version 11.5 (IBM). Spatial profiles of *f*Luc activity were fit to 4-parameter Gaussian profiles using IGOR Pro version 5.05A (Wavemetrics). Significant differences between groups are indicated for $p < 0.05$.

Results

Characterization of cells engineered with a heat-activated and ligand-dependent gene switch to regulate the expression of BMP2

We previously described the development of a heat shock protein (Hsp)- and ligand-inducible gene switch for stringent control of a luciferase reporter or *h*VEGF$_{165}$.[15] Figure 1A summarizes how these gene switches function. Briefly, the human HSP70B promoter initiates transcription of a bimodular transactivator (TA). Each module contains a unique rapamycin-binding domain, and either a DNA-binding domain or a transcriptional activation domain. The modules heterodimerize in the presence of rapamycin or the AP21967 rapalog to form a functional transcription factor. The chimeric TA thereby drives expression of a transgene of interest and also activates its own expression through an autoregulatory loop. Under a regular regimen of dimerizer administration, the gene switch is able to sustain expression of the transgene for 5–8 days following a transient (e.g., ≤30 min) heat shock stimulus.[15] For applications in cartilage and bone regeneration, a stable, clonal cell line was established containing a gene switch regulating BMP2 expression. Cells of this line produced nanogram quantities of BMP2 upon exposure to hyperthermia in the presence of 10 nM rapamycin (Fig. 1B), yielding concentrations of BMP2 in the conditioned medium of ~4 ng/mL and within the cell-scaffold construct of ~15 ng/mL. Conversely, these cells exhibited low background levels of BMP2 production in the absence of thermal stress and/or the dimerizer. These results demonstrate the tight regulation of BMP2 expression achievable using this heat shock- and ligand-inducible gene switch.

A BRE reporter cell line was used to evaluate the bioactivity of BMP2 in conditioned medium from C3H10T½-BMP2 cells (Fig. 1C). Significant increases in *f*Luc activity were detected in BRE reporter cells treated with conditioned media from C3H10T½-BMP2 cells induced by heat treatment at 45°C for 30–45 min in the presence of 10 nM AP21967 compared with controls not subjected to hyperthermia and/or exposed to vehicle (Fig. 1C). This result indicates that induction of the Hsp-based and dimerizer-dependent cell line results in the secretion of bioactive BMP2.

Activation of heat-inducible and ligand-dependent reporter gene expression by focused ultrasound

Induction of cells harboring Hsp-based, rapamycin-dependent gene switches using nonfocused methods of heat delivery such as a hyperthermic water bath, leads to global activation of the monolayer culture or cell-scaffold construct.[15] To achieve spatially-restricted patterns of expression, focused ultrasound was used to control the deposition of energy within 3D cell-fibrin constructs. The ultrasound exposure conditions for generating mild hyperthermia within the constructs were determined using the apparatus shown in Figure 2A. To calibrate the system, ultrasound was applied to cell-free fibrin scaffolds and the temperature at and near the focus of the transducer was measured using an embedded thermocouple. Figure 2B shows typical temperature rises within a scaffold for an acoustic intensity of $I_{SPTA} = 658$ W/cm^2. At the focus of the transducer, a maximum$\Delta T \approx 8$°C was measured after 10 min of ultrasound exposure, and the peakΔT decreased with increasing distance from the focus. These data demonstrate that focused ultrasound can generate mild hyperthermia that is restricted to a millimetric subvolume of a fibrin scaffold.

The next series of experiments measured the ability of focused ultrasound to activate gene expression in C3H10T½-*f*Luc cells suspended in 3D fibrin gels (Fig. 3). For an acoustic intensity of $I_{SPTA} = 754$ W/cm^2, exposure times of 5, 10, and 15 min yielded progressive increases in the projected area and intensity of *f*Luc activity compared with nonirradiated regions of the constructs (Fig. 3A, B). In separate experiments, we found that increases in ultrasound intensity also yielded significant differences in transgene expression. For 5 min duration exposures, acoustic intensities of $I_{SPTA} = 658$–850 W/cm^2 generated significant and substantial increases in *f*Luc activity compared with nonirradiated regions of the construct (Fig. 3C). In addition, exposures at $I_{SPTA} = 850$ W/cm^2 generated larger areas of activation compared with exposures at $I_{SPTA} = 658$ W/cm^2 (Fig. 3D). Ultrasound-activated regions of *f*Luc activity

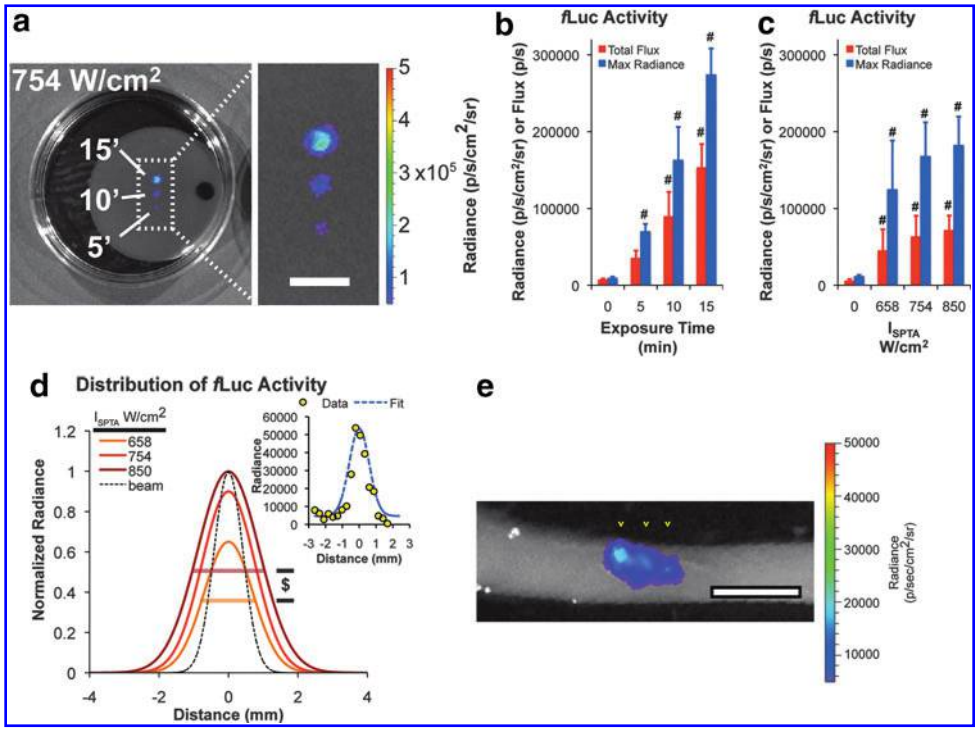

FIG. 3. Spatially restricted activation of gene switch activity using focused ultrasound. **(a)** Time-dependence of induction. Triplicate fibrin scaffolds containing C3H10T½-*f*Luc cells were exposed to focused ultrasound ($I_{SPTA} = 754\ W/cm^2$) for the indicated times before measurement of bioluminescence. Scale bar = 5 mm. **(b)** Quantification of the bioluminescence signals (average radiance and total flux) in nonirradiated and ultrasound-treated regions of the constructs. $^{\#}p < 0.05$ versus nonirradiated. Data are mean ± standard deviation, $n = 3$. **(c)** Ultrasound intensity-dependent activation of C3H10T½-*f*Luc cells. Cell-scaffold constructs were exposed to increasing ultrasound intensities for 5 min ($I_{SPTA} = 0$–$850\ W/cm^2$) and the bioluminescence of treated and nonirradiated regions was quantified 24 h later. $^{\#}p < 0.05$ versus nonirradiated. Data are mean ± standard deviation with $n = 6$. **(d)** Ultrasound intensity-dependent increases in the lateral width of *f*Luc-expressing region. Mean best-fit Gaussian profiles are shown. $ $p < 0.05$ for width of $658\ W/cm^2$ versus $850\ W/cm^2$. Dashed line indicates the geometry of the acoustic beam at the focus. Inset shows typical quality of fit between the measured distribution of *f*Luc activity and the best-fit Gaussian profile. **(e)** A cross section of a cell-fibrin construct treated with three ultrasound exposures (denoted by three yellow arrowheads; 10 min at $I_{SPTA} = 754\ W/cm^2$ for each exposure) focused at different depths (separated longitudinally by 1.5 mm, laterally by 2 mm) within the construct. The incident surface is on the bottom. Scale bar = 5 mm.

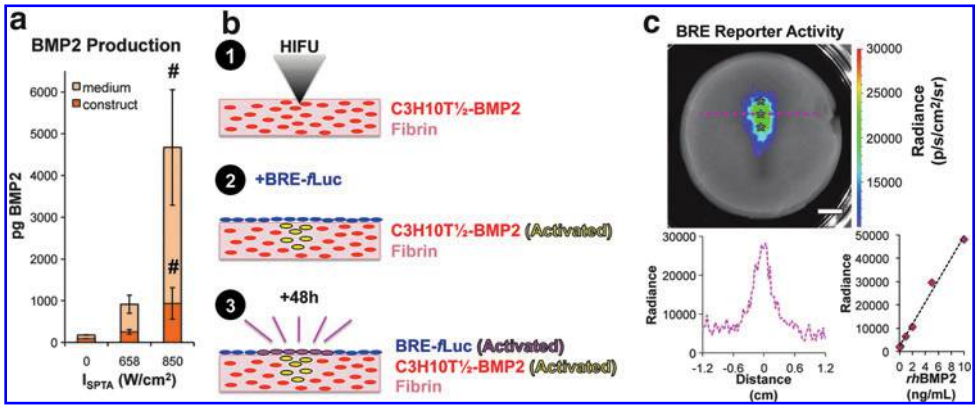

FIG. 4. Ultrasound-induced expression of bioactive BMP2 in cell-fibrin constructs. **(a)** Accumulation of BMP2 in conditioned media (''medium'') and lysates (''construct'') from cell-fibrin constructs exposed to focused ultrasound ($I_{SPTA} = 0$–$850\ W/cm^2$). Irradiated and nonirradiated regions of the constructs were extracted following HIFU exposure and cultured separately. $^{\#}p < 0.05$ versus nonirradiated controls. Data are mean ± standard error of the mean with $n = 12$ for controls and $n = 9$/group for ultrasound-treated samples. **(b)** Schematic describing experimental approach to localizing expression of bioactive BMP2 following HIFU treatment of C3H10T½-BMP2 cells in a fibrin scaffold. **(c)** After localization of BRE reporter activity in cells plated on an ultrasound-treated cell-fibrin construct. Asterisks indicate nominal locations of ultrasound exposure and the pink dashed line denotes line scan region for quantification. Scale bar = 5 mm. Lower panels indicate quantification of BRE reporter cell *f*Luc expression in a line scan across the center of the cell-fibrin construct and a calibration curve showing the relationship between BRE reporter cell *f*Luc expression and treatment with known concentrations of *rh*BMP2.

were found to be restricted along the longitudinal axis of the acoustic beam. By moving the transducer along the longitudinal axis, targeted activation in the third dimension was observed (Fig. 3E). These results indicate that focused ultrasound can activate cells engineered with a heat- and ligand-inducible gene switch in a highly spatially restricted manner. In addition, the magnitude and area of activation may be tuned by the duration and intensity of ultrasound energy delivered at the focus.

Spatially controlled induction of regenerative transgenes using focused ultrasound

To determine whether focused ultrasound could be used to activate expression of a regenerative transgene within a defined spatial volume, cell-fibrin constructs containing C3H10T½-BMP2 cells were examined. Following exposure to HIFU, irradiated and nonirradiated regions were extracted and cultured separately. Irradiated regions of constructs exhibited significant, intensity-dependent increases in BMP2 measured in conditioned medium and lysates compared with nonirradiated regions of the same construct (Fig. 4A). Similar results were obtained after ultrasound activation of cells harboring a gene switch regulating the expression of $h\text{VEGF}_{165}$ (Supplementary Fig. 1; Supplementary Data are available online at www.liebertpub.com/tec), with elevated levels of *h*VEGF detected up to 96 h after irradiation. This is consistent with our previous data describing the dose dependence and kinetics of transgene overexpression following a generalized hyperthermic stimulus.[19] To further define the degree to which BMP2 synthesis was spatially restricted within constructs, BRE-reporter cells were plated on a cell-fibrin construct previously irradiated with focused ultrasound and the pattern of reporter luciferase activity was imaged (experimental approach shown schematically in Fig. 4B). As shown in Figure 4C (upper panel), the BMP2 produced by ultrasound-activated C3H10T½-BMP2 cells was able to generate a highly spatially restricted pattern of BMP signaling. Image analysis revealed that elevated BRE reporter activity dissipated laterally to background levels within 3 mm of the ultrasound focus (Fig. 4C, lower left panel). Based on prior experiments where BRE reporter activity was calibrated against known concentrations of *rh*BMP2 (Fig. 4C, lower right panel), apparent local concentrations of bioactive BMP2 produced by ultrasound-activated C3H10T½-BMP2 cells were in the range of 1–5 ng/mL.

Cell viability and scaffold morphology in ultrasound-irradiated cell-fibrin constructs

Quantitative metabolic assays were used to measure cytotoxic effects of the ultrasound exposures on cells suspended in a fibrin scaffold. No significant differences in metabolic activity were detected for exposure times of 5–15 min at an acoustic intensity of $I_{SPTA} = 754\ W/cm^2$ compared with nonirradiated regions of the construct (Fig. 5A). Similarly, no substantial differences in metabolic activity were detected for acoustic intensities of $I_{SPTA} = 658–850\ W/cm^2$ and an exposure time of 5 min, although a modest (< 7%), but significant, reduction in metabolic activity was detected for $I_{SPTA} = 754\ W/cm^2$ in this experiment (Fig. 5B). These results suggest that the ultrasound exposure times and intensities required to activate cells harboring the heat- and ligand-inducible gene switch had limited cytoxicity.

Confocal microscopy analysis of the cell-fibrin constructs provided insight into localized effects of the focused ultrasound on the cells and scaffold. At the incident surface of the constructs, regions devoid of viable cells were detected and the area of these regions increased with the intensity of the applied ultrasound (Fig. 5C, left panels). In addition to clearance of viable cells, increases in the density of fluorescently tagged fibrinogen—indicative of consolidation of the scaffold—were noted within the focal regions. At short distances distal to the incident surface, however, these effects on the cells and the scaffold were diminished (Fig. 5C, right panels). For example, at an acoustic intensity $I_{SPTA} = 658\ W/cm^2$, the density of viable cells was comparable to that of nonirradiated regions of the construct just 80 μm (~2% of the typical axial dimension of gene activation) distal to the incident surface. Higher intensity ultrasound exposures ($I_{SPTA} = 754$ or $850\ W/cm^2$) led to wider and deeper-penetrating regions of cell clearance and scaffold consolidation. In summary, application of focused ultrasound at energies capable of inducing transgene expression had only minor effects on cell viability.

To evaluate the *in vivo* response of cells engineered with a heat- and ligand-inducible gene switch, focused ultrasound was applied to subcutaneous implants composed of C3H10T½-*f*Luc cells in a fibrin scaffold. Twenty-four hours after application of ultrasound, substantial increases *f*Luc expression was observed in the irradiated region, whereas very little bioluminescent signal was observed in nonirradiated control implants (Fig. 6A). Histologic sections of control and ultrasound-treated implants revealed little difference in cell or tissue morphology, indicating that the acoustic energy did not incur damage to the implant and tissues near the focus (Fig. 6B). These results demonstrate the potential for focused ultrasound to selectively activate heat shock- and ligand-inducible gene switches *in vivo*. However, considerable optimization of ultrasound dosing and duration will be required before *in vivo* studies can be initiated to control the formation of vasculature or bone.

Discussion

BMPs have demonstrated efficacy in stimulating bone formation in animal models and human clinical applications, but the supraphysiologic doses of recombinant protein required are associated with systemic side effects such as inflammation, heterotopic ossification, and, in some cases, cancer.[14] Advanced materials for controlling the release of regenerative growth factors show some promise in prolonging and localizing BMP activity to improve bone healing,[20–22] but these platforms are generally limited to first-order release kinetics that preclude reconstitution of more complex kinetic profiles such as those that occur during development. Here, we demonstrate a method of actively regulating the release of regenerative growth factors in both time and space through the targeted application of focused ultrasound to cell-fibrin constructs engineered with a ligand-dependent, heat-inducible gene expression system. Regions of transgene expression as small as ~ $30\ mm^3$ were measured in our studies, and the amplitude and volume of transgene expression could be tuned by the acoustic intensity or exposure time.

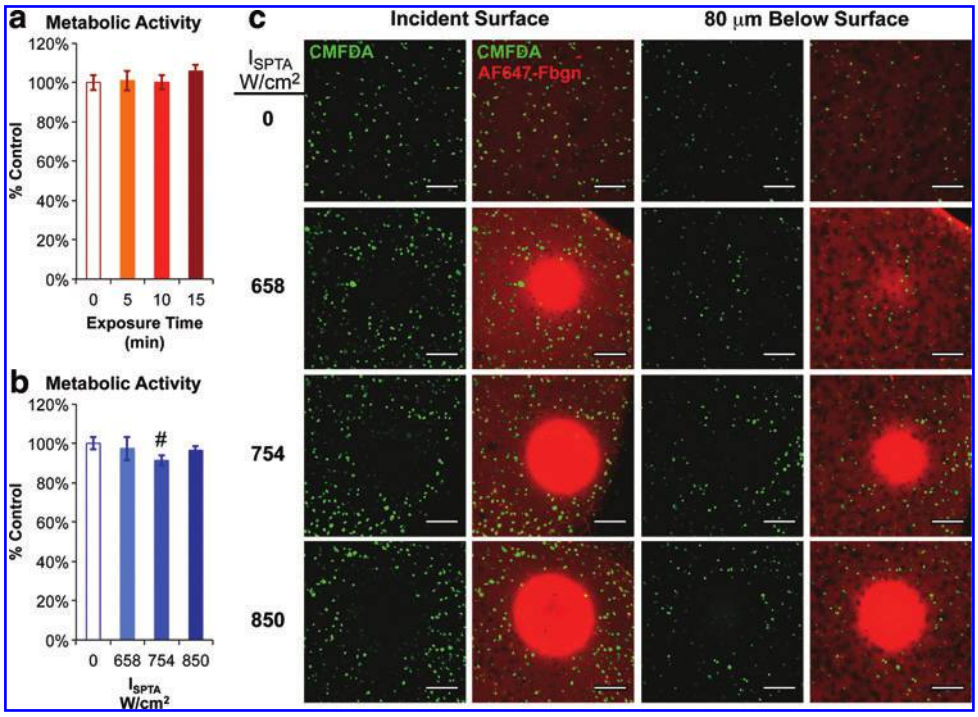

FIG. 5. Viability and morphology of cell-fibrin constructs exposed to focused ultrasound. **(a)** Metabolic activity of portions of cell-fibrin constructs treated with focused ultrasound for increasing times (0–15 min., $I_{SPTA} = 754$ W/cm^2). No differences in metabolic activity measured using an alamarBlue dye reduction assay were detected. Data are mean ± standard deviation with $n = 9$ for controls and $n = 3$/group for ultrasound-treated samples and are expressed as percent control fluorescence of cells not exposed to ultrasound. **(b)** Metabolic activity of cell-fibrin constructs treated for 5 min with increasing ultrasound intensities ($I_{SPTA} = 0$–850 W/cm^2). $^{\#}p < 0.05$ versus nonirradiated controls. Data are mean ± standard deviation with $n = 9$ for controls and $n = 6$/group for ultrasound-treated samples. **(c)** Confocal microscopic images of viable cells (labeled with CMFDA, green) and fibrin scaffold morphology (labeled with AlexaFluor647-fibrinogen, AF647-Fbgn, red) in control and ultrasound-treated regions (10 min, $I_{SPTA} = 0$–850 W/cm^2) of cell-fibrin constructs. Left images captured at the surface of the construct incident to the acoustic beam. Right images captured 80 μm distal from the incident surface. Scale bar = 250 μm. Color images available online at www.liebertpub.com/tec

Both nonfocused and focused ultrasound have been previously used to activate expression of Hsp-based gene expression systems.[19,23,24] These studies demonstrated the potential for ultrasound to activate the heat shock pathway and to target the overexpression of either a reporter gene such as *f*Luc or a cytotoxic transgene such as Fas ligand under the direct control of HSP70 gene promoters. We adapted this approach for use with a dual requirement gene expression system that provides durable expression of regenerative transgenes such as BMP2 and *h*VEGF$_{165}$. In contrast to systems exclusively controlled by HSP promoters, the heat-activated and ligand-dependent gene switch is engineered to avoid inadvertent activation and provide sustained expression of the transgene (i.e., >1–2 days), which is important for growth factor-stimulated bone or cartilage formation. This is also the first study to demonstrate the use of focused ultrasound to stimulate temporal control over regenerative factor synthesis in engineered tissues.

The acoustic intensities and exposure times required to activate transgene expression in cells suspended in the fibrin

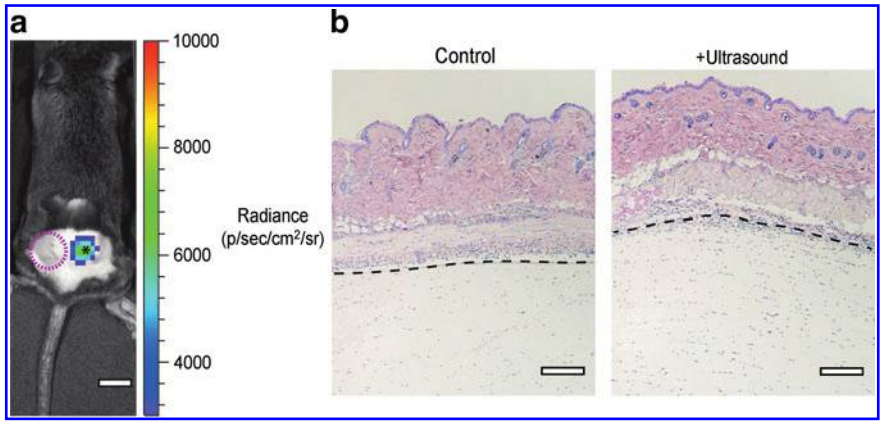

FIG. 6. *In vivo* activation of heat shock- and ligand-inducible gene switch activity with focused ultrasound. **(a)** Bioluminescence imaging of a representative animal with control (encircled by pink dashed line) and ultrasound-irradiated ($I_{SATA} = 658$ W/cm^2 for 10 min; asterisk) cell-fibrin subcutaneous implants. Image was captured 24 h following ultrasound exposure. Scale bar = 10 mm. **(b)** Hematoxylin and eosin staining of histologic sections of subcutaneous implants following ultrasound exposure. Dashed line indicates implant–skin interface. Scale bars = 50 μm.

scaffold are rather high relative to those used in typical imaging instruments, but low compared with other therapeutic ultrasound modalities. The maximum mechanical index (MI, an indicator for the potential of ultrasound to induce cavitation; defined as $P_R/\sqrt{\text{frequency}}$) permitted by the FDA for ultrasound imaging instruments is 1.5, the range of mechanical indices used in the current study was 2.7–3.0. The FDA does, however, permit the application of higher MI ultrasound energies for therapeutic purposes (e.g., MRI-guided HIFU ablation procedures) and we found no evidence of cavitation, such as homogenization of the cell-scaffold construct, in our experiments. The examined intensities bracketed the minimum required to trigger transgene expression and the maximum allowable without perforating the Tegaderm membranes used in the experimental setup. Although ultrasound exposures of $I_{SPTA} = 658\ W/cm^2$ did not trigger substantial cytotoxicity or damage to the fibrin scaffold, some clearance of viable cells and consolidation of the fibrin scaffold at the incident surface was observed. Acoustic radiation force or fluid streaming may be responsible for such effects.[25,26] Speed of sound measurements indicated that the acoustic attenuation of the fibrin scaffold is very low, ~ 0.05 dB/cm/MHz or 5–10% of the attenuation of soft tissue,[27] indicating that much of the ultrasound energy passes through the constructs without being absorbed or scattered and converted to heat. In unpublished studies, we found that increasing the density of the fibrin scaffold by adding bovine serum albumin, insoluble elastin particles, or more clottable protein increased the attenuation by 2–10-fold, suggesting that the scaffold can be modified to attenuate more of the ultrasound energy. Studies are currently underway to identify combinations of higher attenuating scaffolds and lower intensity acoustic exposures that provide robust activation of transgene expression and reduce adverse effects on cell viability and scaffold morphology. Tuning the acoustic beam geometry, frequency, and delivery mode (continuous vs. pulsed) are alternative approaches to improving energy deposition and minimizing adverse effects within the cell-scaffold constructs.

The use of rapamycin as a dimerizing agent could potentially interfere with processes such as proliferation required for regeneration. This naturally derived compound acts as an inhibitor of the mammalian target of rapamycin pathway that regulates many growth-related processes. Indeed, rapamycin inhibits the proliferation and differentiation of a preosteoblast cell line and primary bone marrow-derived stromal cells.[28] Previous studies in our lab, however, have shown that the doses of rapamycin required for activation of rapamycin-dependent gene switches do not block bone formation *in vivo*.[11] In addition, nonimmunosuppresive synthetic analogs of rapamycin, such as AP21967, retain high affinity for the FRB and FKBP domains found in transactivator modules and thus can serve as reliable dimerizing agents[29] that exhibit much lower anti-proliferative activity than rapamycin.[30]

Although the heat-activated gene switches described in our study used rapamycin/rapamycin analogues as activating ligand, this system can be adapted to the use of different ligands, thereby providing control over a range of regenerative factors. For example, we previously described a mifepristone-dependent heat shock-inducible gene switch[31] that could be adapted for ultrasound-mediated regulation of an additional osteogenic factor, such as fibroblast growth factor 2 or parathyroid hormone, which would augment the regenerative effects of VEGF or BMP2. Previous attempts at combining delivery of growth factors have yielded modestly improved, but ultimately disappointing results compared with monotherapies in animal models of bone healing.[19,32–35] With advanced methods of regulating the timing and localization of transgene expression, combination therapies may prove substantially more effective than single growth factor treatments for applications in regenerative medicine.

Stable cell lines harboring the heat shock-inducible and ligand-dependent gene switches were used in the current studies for convenience and consistency, but translation of this technology to the clinic will require reliable methods for efficient gene transfer to target cell populations (e.g., autologous progenitor cells). Nonviral methods such as nucleofection, an electroporation-based gene transfer technique, has been used to deliver plasmids encoding BMPs into human mesenchymal progenitor cells with moderate success.[36] Viral vectors are currently the most efficient means of delivering transgenes into cells, but often carry risk of immunogenicity and transformation of infected cells. AAV, in contrast, are not pathogenic or immunogenic and neither recombinant AAV (rAAV) nor its parental virus has been shown to induce malignancies in humans. These features, combined with the stability of the transgenic expression provided by rAAV and their ability to transduce a variety of cells confer exceptional value to this biological tool in gene therapies intended to promote tissue regeneration.[37–39]

The results of our *in vivo* study provide proof of principle that ultrasound can be safely used to target and activate gene switch-engineered cells placed within the body. However, induction of bone or vasculature will require the identification of optimal conditions for stimulating BMP or VEGF expression *in vivo*. In addition, clinical grade image-guided ultrasound instruments will be required to tightly control the deposition of acoustic energy into implanted cell-scaffold grafts. Magnetic resonance thermography is the most commonly used method of imaging ultrasound-generated hyperthermia within the body, and provides real-time control over the deposition of acoustic energy based on a target temperature for a target volume of tissue. Therefore, many of the tools are in place to implement an ultrasound-activated cell-based therapy for the regeneration of large tissue defects.

Conclusions

This study demonstrates that focused ultrasound can activate cells harboring a heat activated- and ligand-dependent gene switch to induce the expression of a regenerative growth factor within a precisely defined 3D space. Ultrasound had limited cytotoxicity on targeted cells within scaffolds and induced only minor structural damage to the hydrogel scaffold. This approach to controlling the spatial and temporal patterns of growth factor expression should have broad utility in basic and applied studies of tissue regeneration.

Acknowledgments

This research was supported by the National Institutes of Health (NIH) grant R01DE013386-09 (RTF), Department of

Defense grant OR090134 (RTF), and grant PI12/01698 (NV) from Fondo de Investigaciones Sanitarias (Spain). NV and FM-S were supported by programs I2 and Sara Borrell, respectively, from Comunidad de Madrid and Fondo de Investigaciones Sanitarias (Spain). CGW was supported by a postdoctoral fellowship through NIH training grant T32DE007057-34. AMB was supported by a graduate student fellowship from the National Science Foundation. The gifts of BRE reporter cells from Dr. Delphine Logeart-Avramoglou (Laboratoire Biomecanique et Biomateriaux Ostéo-Articulaires) and AP21967 from ARIAD Pharmaceuticals are also gratefully acknowledged.

Disclosure Statement

R.V. declares the following conflict of interest: he is the Founder and C.E.O. of HSF Pharmaceuticals S.A. None of the other authors has conflicts of interest related to this work.

References

1. Maes, C., and Cermeliet, G. Vascular and nonvascular roles of VEGF in bone development. In: Ruhrberg, C., ed. VEGF in Development. Springer, Austin, pp. 79–90, 2008.
2. Choi, K-S., Lee, C., Maatouk, D.M., and Harfe, B.D. Bmp2, Bmp4 and Bmp7 are co-required in the mouse AER for normal digit patterning but not limb outgrowth. PLoS One **7,** e37826, 2012.
3. Bénazet, J-D., Bischofberger, M., Tiecke, E., Gonçalves, A., Martin, J.F., Zuniga, A., *et al.* A self-regulatory system of interlinked signaling feedback loops controls mouse limb patterning. Science **323,** 1050, 2009.
4. Ferguson, C., Alpern, E., Miclau, T., and Helms, J. Does adult fracture repair recapitulate embryonic skeletal formation? Mech Dev **87,** 57, 1999.
5. Gerstenfeld, L.C., Cullinane, D.M., Barnes, G.L., Graves, D.T., and Einhorn, T.A. Fracture healing as a post-natal developmental process: molecular, spatial, and temporal aspects of its regulation. J Cell Biochem **88,** 873, 2003.
6. Yu, Y.Y., Lieu, S., Lu, C., and Colnot, C. Bone morphogenetic protein 2 stimulates endochondral ossification by regulating periosteal cell fate during bone repair. Bone **47,** 65, 2010.
7. Rutherford, R.B., Moalli, M., Franceschi, R.T., Wang, D., Gu, K., and Krebsbach, P.H. Bone morphogenetic protein-transduced human fibroblasts convert to osteoblasts and form bone *in vivo*. Tissue Eng **8,** 441, 2002.
8. Baltzer, A., Lattermann, C., Whalen, J., Wooley, P., Weiss, K., Grimm, M., *et al.* Genetic enhancement of fracture repair: healing of an experimental segmental defect by adenoviral transfer of the BMP-2 gene. Gene Ther **7,** 734, 2000.
9. Lieberman, J.R., Daluiski, A., Stevenson, S., Wu, L., McAllister, P., Lee, Y.P., *et al.* The effect of regional gene therapy with bone morphogenetic protein-2-producing bone-marrow cells on the repair of segmental femoral defects in rats. J Bone Joint Surg Am **81,** 905, 1999.
10. Moutsatsos, I.K., Turgeman, G., Zhou, S., Kurkalli, B.G., Pelled, G., Tzur, L., *et al.* Exogenously regulated stem cell-mediated gene therapy for bone regeneration. Mol Ther **3,** 449, 2001.
11. Koh, J-T., Ge, C., Zhao, M., Wang, Z., Krebsbach, P.H., Zhao, Z., *et al.* Use of a stringent dimerizer-regulated gene expression system for controlled BMP2 delivery. Mol Ther **14,** 684, 2006.
12. Axelrad, T.W., Steen, B., Lowenberg, D.W., Creevy, W.R., and Einhorn, T.A. Heterotopic ossification after the use of commercially available recombinant human bone morphogenetic proteins in four patients. J Bone Joint Surg Br **90,** 1617, 2008.
13. Dmitriev, A.E., Castner, S., Lehman, R.A., Ling, G.S.F., and Symes, A.J. Alterations in recovery from spinal cord injury in rats treated with recombinant human bone morphogenetic protein-2 for posterolateral arthrodesis. J Bone Joint Surg **93,** 1488, 2011.
14. Carragee, E.J., Hurwitz, E.L., and Weiner, B.K. A critical review of recombinant human bone morphogenetic protein-2 trials in spinal surgery: emerging safety concerns and lessons learned. Spine J **11,** 471, 2011.
15. Martín-Saavedra, F.M., Wilson, C.G., Voellmy, R., Vilaboa, N., and Franceschi, R.T. Spatiotemporal control of vascular endothelial growth factor expression using a heat-shock-activated, rapamycin-dependent gene switch. Hum Gene Ther Methods **24,** 160, 2013.
16. Ranjan, A., Jacobs, G.C., Woods, D.L., Negussie, A.H., Partanen, A., Yarmolenko, P.S., *et al.* Image-guided drug delivery with magnetic resonance guided high intensity focused ultrasound and temperature sensitive liposomes in a rabbit Vx2 tumor model. J Control Release **158,** 487, 2012.
17. Partanen, A., Tillander, M., Yarmolenko, P.S., Wood, B.J., Dreher, M.R., and Kohler, M.O. Reduction of peak acoustic pressure and shaping of heated region by use of multifoci sonications in MR-guided high-intensity focused ultrasound mediated mild hyperthermia. Med Phys **40,** 013301, 2013.
18. Logeart-Avramoglou, D., Bourguignon, M., Oudina, K., Dijke Ten, P., and Petite, H. An assay for the determination of biologically active bone morphogenetic proteins using cells transfected with an inhibitor of differentiation promoter-luciferase construct. Anal Biochem **349,** 78, 2006.
19. Kruse, D.E., Mackanos, M.A., O'Connell-Rodwell, C.E., Contag, C.H., and Ferrara, K.W. Short-duration-focused ultrasound stimulation of Hsp70 expression *in vivo*. Phys Med Biol **53,** 3641, 2008.
20. Kempen, D.H.R., Lu, L., Heijink, A., Hefferan, T.E., Creemers, L.B., Maran, A., *et al.* Effect of local sequential VEGF and BMP-2 delivery on ectopic and orthotopic bone regeneration. Biomaterials **30,** 2816, 2009.
21. la Riva De, B., Sánchez, E., Hernández, A., Reyes, R., Tamimi, F., López-Cabarcos, E., *et al.* Local controlled release of VEGF and PDGF from a combined brushite-chitosan system enhances bone regeneration. J Control Release **143,** 45, 2010.
22. Kolambkar, Y.M., Boerckel, J.D., Dupont, K.M., Bajin, M., Huebsch, N., Mooney, D.J., *et al.* Spatiotemporal delivery of bone morphogenetic protein enhances functional repair of segmental bone defects. Bone **49,** 485, 2011.
23. Smith, R.C., Machluf, M., Bromley, P., Atala, A., and Walsh, K. Spatial and temporal control of transgene expression through ultrasound-mediated induction of the heat shock protein 70B promoter *in vivo*. Hum Gene Ther **13,** 697, 2002.
24. Deckers, R., Quesson, B., Arsaut, J., Eimer, S., Couillaud, F., and Moonen, C.T.W. Image-guided, noninvasive, spatiotemporal control of gene expression. Proc Natl Acad Sci U S A **106,** 1175, 2009.

25. Walker, W.F. Internal deformation of a uniform elastic solid by acoustic radiation force. J Acoust Soc Am **105,** 2508, 1999.
26. Sarvazyan, A.P., Rudenko, O.V., and Nyborg, W.L. Biomedical applications of radiation force of ultrasound: historical roots and physical basis. Ultrasound Med Biol **36,** 1379, 2010.
27. Goss, S.A., Johnston, R.L., and Dunn, F. Compilation of empirical ultrasonic properties of mammalian tissues. II J Acoust Soc Am **68,** 93, 1980.
28. Singha, U.K., Jiang, Y., Yu, S., Luo, M., Lu, Y., Zhang, J., *et al.* Rapamycin inhibits osteoblast proliferation and differentiation in MC3T3-E1 cells and primary mouse bone marrow stromal cells. J Cell Biochem **103,** 434, 2008.
29. Pollock, R., Giel, M., Linher, K., and Clackson, T. Regulation of endogenous gene expression with a small-molecule dimerizer. Nat Biotechnol **20,** 729, 2002.
30. Indraccolo, S., Moserle, L., Tisato, V., Gola, E., Minuzzo, S., Roni, V., *et al.* Gene therapy of ovarian cancer with IFN-alpha-producing fibroblasts: comparison of constitutive and inducible vectors. Gene Ther **13,** 953, 2006.
31. Vilaboa, N., Fenna, M., Munson, J., Roberts, S.M., and Voellmy, R. Novel gene switches for targeted and timed expression of proteins of interest. Mol Ther **12,** 290, 2005.
32. Peng, H., Wright, V., Usas, A., Gearhart, B., Shen, H-C., Cummins, J., *et al.* Synergistic enhancement of bone formation and healing by stem cell-expressed VEGF and bone morphogenetic protein-4. J Clin Invest **110,** 751, 2002.
33. Peng, H., Usas, A., Olshanski, A., Ho, A.M., Gearhart, B., Cooper, G.M., *et al.* VEGF improves, whereas sFlt1 inhibits, BMP2-induced bone formation and bone healing through modulation of angiogenesis. J Bone Miner Res **20,** 2017, 2005.
34. Patel, Z.S., Young, S., Tabata, Y., Jansen, J.A., Wong, M.E.K., and Mikos, A.G. Dual delivery of an angiogenic and an osteogenic growth factor for bone regeneration in a critical size defect model. Bone **43,** 931, 2008.
35. Young, S., Patel, Z.S., Kretlow, J.D., Murphy, M.B., Mountziaris, P.M., Baggett, L.S., *et al.* Dose effect of dual delivery of vascular endothelial growth factor and bone morphogenetic protein-2 on bone regeneration in a rat critical-size defect model. Tissue Eng Part A **15,** 2347, 2009.
36. Aslan, H., Zilberman, Y., Arbeli, V., Sheyn, D., Matan, Y., Liebergall, M., *et al.* Nucleofection-based *ex vivo* nonviral gene delivery to human stem cells as a platform for tissue regeneration. Tissue Eng **12,** 877, 2006.
37. Yazici, C., Takahata, M., Reynolds, D.G., Xie, C., Samulski, R.J., Samulski, J., *et al.* Self-complementary AAV2.5-BMP2-coated femoral allografts mediated superior bone healing versus live autografts in mice with equivalent biomechanics to unfractured femur. Mol Ther **19,** 1416, 2011.
38. Dupont, K.M., Boerckel, J.D., Stevens, H.Y., Diab, T., Kolambkar, Y.M., Takahata, M., *et al.* Synthetic scaffold coating with adeno-associated virus encoding BMP2 to promote endogenous bone repair. Cell Tissue Res **347,** 575, 2012.
39. Ishihara, A., Bartlett, J.S., and Bertone, A.L. Inflammation and immune response of intra-articular serotype 2 adeno-associated virus or adenovirus vectors in a large animal model. Arthritis **2012,** 735472, 2012.

Address correspondence to:
Renny T. Franceschi, PhD
Department of Periodontics and Oral Medicine
Center for Craniofacial Regeneration
University of Michigan School of Dentistry
1011 N. University Avenue
Ann Arbor, MI 48109-1078

E-mail: rennyf@umich.edu

Received: August 18, 2013
Accepted: January 7, 2014
Online Publication Date: March 11, 2014

This article has been cited by:

1. M. S. Aw, L. Paniwnyk. 2017. Overcoming T. gondii infection and intracellular protein nanocapsules as biomaterials for ultrasonically controlled drug release. *Biomaterials Science* **5**:10, 1944-1961. [Crossref]
2. Mario L. Fabiilli, Rahul A. Phanse, Alexander Moncion, J. Brian Fowlkes, Renny T. Franceschi. 2016. Use of Hydroxyapatite Doping to Enhance Responsiveness of Heat-Inducible Gene Switches to Focused Ultrasound. *Ultrasound in Medicine & Biology* **42**:3, 824-830. [Crossref]
3. Diane Dalecki, Denise C. Hocking. Advancing Ultrasound Technologies for Tissue Engineering 1101-1126. [Crossref]
4. Julia E. Samorezov, Eben Alsberg. 2015. Spatial regulation of controlled bioactive factor delivery for bone tissue engineering. *Advanced Drug Delivery Reviews* **84**, 45-67. [Crossref]
5. Diane Dalecki, Denise C. Hocking. 2015. Ultrasound Technologies for Biomaterials Fabrication and Imaging. *Annals of Biomedical Engineering* **43**:3, 747-761. [Crossref]
6. Miguel Padial-Molina, Francisco O'Valle, Alejandro Lanis, Francisco Mesa, David M. Dohan Ehrenfest, Hom-Lay Wang, Pablo Galindo-Moreno. 2015. Clinical Application of Mesenchymal Stem Cells and Novel Supportive Therapies for Oral Bone Regeneration. *BioMed Research International* **2015**, 1-16. [Crossref]
7. Francisco M. Martin-Saavedra, Virginia Cebrian, Leyre Gomez, Daniel Lopez, Manuel Arruebo, Christopher G. Wilson, Renny T. Franceschi, Richard Voellmy, Jesus Santamaria, Nuria Vilaboa. 2014. Temporal and spatial patterning of transgene expression by near-infrared irradiation. *Biomaterials* **35**:28, 8134-8143. [Crossref]